Chinese Chemical Letters 31 (2020) 779–782

Contents lists available at ScienceDirect

Chinese Chemical Letters

journal homepage: www.elsevier.com/locate/cclet

Communication

Thermal benzene activation by 3d transition metal (Sc-Cu) oxide cations

Jiatong Cui[a], Yue Zhao[a], Ming Wang[a], Shanshan Wang[b], Jiabi Ma[a,*]

[a] *Key Laboratory of Cluster Science of Ministry of Education, Beijing Key Laboratory of Photoelectronic/Electrophotonic Conversion Materials, School of Chemistry and Chemical Engineering, Beijing Institute of Technology, Beijing 100081, China*
[b] *Analysis & Testing Center, Beijing Institute of Technology, Beijing 100081, China*

ARTICLE INFO

Article history:
Received 16 April 2019
Received in revised form 6 May 2019
Accepted 7 May 2019
Available online 7 May 2019

Keywords:
Gas-phase reactions
Transition metal oxide cations
Benzene
Mass spectrometry
Ion-molecular reaction

ABSTRACT

Considering the importance and complexity of benzene oxidation on mineral oxide aerosol surfaces in the atmosphere, gas-phase 3d-transition metal oxide cations were used as models of active sites on mineral oxide aerosols to mimic the corresponding reactions. The various cations have been prepared by laser ablation and reacted with benzene in a linear ion trap reactor. Of the 103 systematically investigated cations, 39 clusters can oxidize benzene at room temperature. In addition to the adsorption channel, other five types of reaction channels were observed, including dehydrogenation of C_6H_6, charge exchange, hydrogen atom transfer, oxygen atom transfer, and the formation of $C_6H_5O^•$ radical, among which the first two pathways are prevalent and the formation of $C_6H_6O^+$ cations has not been reported in literature. The insight into the benzene oxidation reactions derived from the gas-phase model systems is helpful to build a detailed picture of oxidative mechanisms of C_6H_6 and its derivatives over corresponding mineral oxide aerosols.

In the atmosphere, aromatic hydrocarbons are an important fraction of volatile organic compounds (VOCs) [1], among which benzene (C_6H_6) is the simplest but ubiquitous pollutant. Mineral dust particles including various metal oxides provide adsorption sites of VOCs, and reactive surfaces for heterogeneous reactions [2,3]. The oxidation reactions of VOCs such as benzene can result in the formation of oxygenated products with lower volatilities and these highly-oxidized compounds are quite important to the generation of secondary organic aerosols (SOAs) [4,5]. SOAs are one of the major components throughout the haze-fog episodes in China [6], and particle-phase reactions are one of important processes of the SOA formation [7,8]. Vanadium, manganese, nickel, chromium, and copper are abundant heavy metals found in the atmosphere in the north of China [9,10], and there are various reactive oxide species on the mineral oxide surfaces, which are key species of atmospheric chemistry [11]. Apart from the above mentioned transition metal oxides, Fe_2O_3 as well as TiO_2 are also typical mineral aerosols. It is quite desirable to obtain the detailed reaction kinetic data and reaction mechanisms to understand the intrinsic properties of reaction centers of mineral dust aerosols at a molecular level and offer basic parameters for atmospheric models. However, the enormous complexities of environmental factors and relative reaction products render the reactions as well as the nature of active centers obscure.

Gas-phase experiments conducted under properly defined conditions provide an ideal arena for probing the energtics and kinetics of a reaction at a strictly molecular level [12–22]. Investigations on benzene oxidation by gas-phase ions and clusters gives fundamental insights for how benzene molecules can be activated and the nature of active sites. There are some reports about the reactions of metal ions [23–38], metal clusters [32,36,39], and several transition metal oxide ions [40–43] with benzene. Large amount of experimental efforts have been devoted to the study of 3d transition metal atoms (M = Sc-Ni) interacting with C_6H_6, and sandwich and rice-ball structures for $M_n(C_6H_6)_m$ were observed [25]. In addition, the adsorption, C—H bond activation [44], dehydrogenation and dissociation processes [24,45,46] of benzene molecules mediated by gas-phase ions and clusters were also reported. Notably, there is a lack of clear picture about the reactivity of small 3d transition metal oxide cluster (TMOC) cations toward C_6H_6 in the literature, which is useful in elucidating compositions of reactive clusters, the reaction trends and the possible oxidative ability of mineral aerosols.

In this study, we systematically investigate 103 reactions of first-row transition metal oxide cations $M_xO_y^+$ (M = Sc-Cu, x = 1–6) with C_6H_6 in the linear ion trap at near room temperature. Thirty-

---

[*] Corresponding author.
E-mail address: majiabi@bit.edu.cn (J. Ma).

https://doi.org/10.1016/j.cclet.2019.05.015

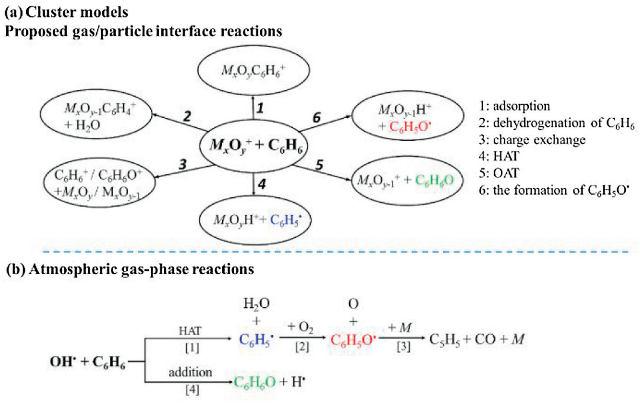

Scheme 1. Simplified reaction channels for the reactions of $M_xO_y^+$ (M = Sc-Cu) cluster cations (a) and atmospheric $OH^•$ radicals (b) with benzene.

nine clusters show high reactivity toward benzene and display up to six primary reaction channels, as shown in Scheme 1a: 1) adsorption channel, 2) dehydrogenation of C_6H_6, 3) charge exchange, 4) hydrogen atom transfer (HAT), 5) oxygen atom transfer (OAT) and 6) the formation of $C_6H_5O^•$ radical. In addition to $M_xO_yC_6H_6^+$, five types of oxidation products are generated during these reactions, that is, C_6H_4 unit, $C_6H_5^•$ (phenyl) radical, $C_6H_6O_{0,1}^+$ cations, $C_6H_6O^•$ and $C_6H_5O^•$ radical. The adsorption channel exists in most of the investigated cluster cations under our experimental conditions, except for ScO_3^+, MnO_4^+ and other 25 inert clusters (Table S1 in Supporting information), and this pathway will not be included in the following discussion. Generally speaking, only series of scandium oxide clusters and vanadium oxide clusters exhibit similar reactivity toward benzene in the 39 reactive 3d TMOC cations; however, more than two types of reactions coexist in other 3d TMOCs. $Co_xO_y^+$ and $Cr_xO_y^+$ cations exhibit variety of the products in the reactions with C_6H_6. The number of reactive $Mn_xO_y^+$ and $Ni_xO_y^+$ clusters is the least. The detailed reaction channels will be discussed in the following.

As shown in Fig. 1 and Fig. S1 (Supporting information), dehydrogenation of C_6H_6 is prevalent in the C_6H_6 oxidation reactions mediated by the reactive metal oxide cations, except for $Sc_xO_y^+$ clusters. The *pseudo*-first order rate coefficients (k_1) [47], which were estimated on the basis of a least-square fitting procedure (Fig. S2 in Supporting information), and the reaction efficiencies ($\Phi = k_1/k_{calc}$; k_{calc} is the theoretical collision rate [48,49]) for these reactions are given in Table 1 and Table S2 (Supporting information). Among the investigated clusters, $Ti_2O_4^+$, $(V_2O_5)_{1-3}^+$, $(V_2O_5)_{0-1}VO_3^+$ [47] $Cr_xO_y^+$ (x,y = 1,2; 2,5; 2,6; 3,2; 3,8), $Mn_2O_3^+$, FeO_4^+, $Fe_2O_3^+$, $Co_xO_y^+$ (x,y = 2,2; 2,5; 3,4; 4,5; 5,7), $Ni_5O_5^+$, as well as $Cu_5O_3^+$ and $Cu_6O_4^+$ can induce dehydrogenation of C_6H_6, with the formation of $M_xO_{y-1}C_6H_4^+$ and H_2O. The estimated rate constants varied from 10^{-9} cm^3 molecule^{-1} s^{-1} to 10^{-10} cm^3 molecule^{-1} s^{-1}, and branching ratios (BRs) of this channel dramatically changes from 1.3% for Cr_2O_6/C_6H_6 to 78% for $V_3O_8^+/C_6H_6$ [50]. More information of reactivity and reaction channels is shown in Fig. 2. Based on the reported B3LYP-calculated results for the reactions of $V_2O_5^+$ and VO_3^+ with C_6H_6, the dehydrogenation pathway proceeds by two steps of C—O bond making and two steps of hydrogen atom abstraction alternately, with the formation of OH moiety and H_2O unit successively [50]. The formed C_6H_4 unit is bonded with two oxygen atoms of oxide clusters by forming a ···—M—O—C—C—O—··· ring in the product [50]. Similar reaction mechanisms may be followed for other reactive TMOCs. Normally, a small change in cluster composition can completely change the reactive properties of the clusters [51,52]. Herein, the dehydrogenation of C_6H_6 generally exists in various 3d TMOC cations, and the reactive clusters contain both of oxygen-rich and oxygen-poor ones. Like $Cr_3O_2^+$, which is very oxygen deficient, can even offer one oxygen atom to form H_2O unit in the C_6H_6 oxidation reactions. Unlike the reactions of stoichiometric early TMOC cations with CH_4 [53], no uniform structural compositions can be summed up for these reactive 3d TMOCs. In addition, the dehydrogenation of C_6H_6 is one of the major channels (BR > 25%) in most of the investigated reactions. In literature, there are some oxide ions which also can bring about the dehydrogenation of C_6H_6, such as FeO^+ [54], MnO^+ [40], V_2O_5 and $(V_2O_5)_{0-2}VO_3$ [42], and the branching ratios of this channel for MnO^+ and FeO^+ are only 10% and 5%, respectively.

In addition to dehydrogenation of C_6H_6, charge exchange channel is also observed in many investigated 3d TMOC cations, and two kinds of products $C_6H_6^+$ and $C_6H_6O^+$ are present, as shown in Fig. 1 and Fig. S1. For $V_3O_8^+$, $V_5O_{13}^+$, $Cr_2O_6^+$, $Cr_4O_{11}^+$ and $Ni_4O_5^+$, the charge exchange channel is concomitant with the OAT channel, resulting to the formation of $C_6H_6O^+$ ions as the products of the reactions with C_6H_6. For the reactions of $(V_2O_5)_{1-3}^+$, $Cr_xO_y^+$ (x, y = 1,2; 2,5; 2,6; 3,2; 3,8; 4,10; 4,11), MnO_2^+ and $Co_xO_y^+$ (x,y = 1,4; 2,3; 2,5) with C_6H_6, $C_6H_6^+$ cations are the reaction products. The charge transfer happens when cluster cations collide with benzene molecules [50], and this channel is closely related to the ionization energies (IEs) of benzene, phenol and relative neutral TMOCs. If $C_6H_6^+$ is present in the mass spectra, the IEs of neutral TMOCs can be assigned as larger than that of C_6H_6. Mass discrimination effect due to large mass difference between $C_6H_6O_{0,1}^+$ and oxide clusters makes it difficult to exhibit the precise intensity of $C_6H_6^+$ in some reactions, and this phenomenon is more serious for larger clusters. Thus, it is hard to accurately compare the productions of $C_6H_6O_{0,1}^+$ for the reactions of the small clusters with those of the larger clusters. This charge exchange channel also takes place in the reactions of benzene with Co^+, Cu^+, Nb^+ [55] and Au^+ [37] ions, forming $C_6H_6^+$ cations. However, the pathway of generating $C_6H_6O^+$ has not been reported in the studies of C_6H_6 oxidation reaction mediated by gas-phase clusters. In the atmosphere, charge exchange reactions, such as $H + O^+ \rightarrow H^+ + O$ and $O_2^+ + NO \rightarrow O_2 + NO^+$, have been studied extensively [56]. From our gas-phase reactions, one may expect that this reaction type may also exist between mineral oxides and some VOC molecules, such as C_6H_6.

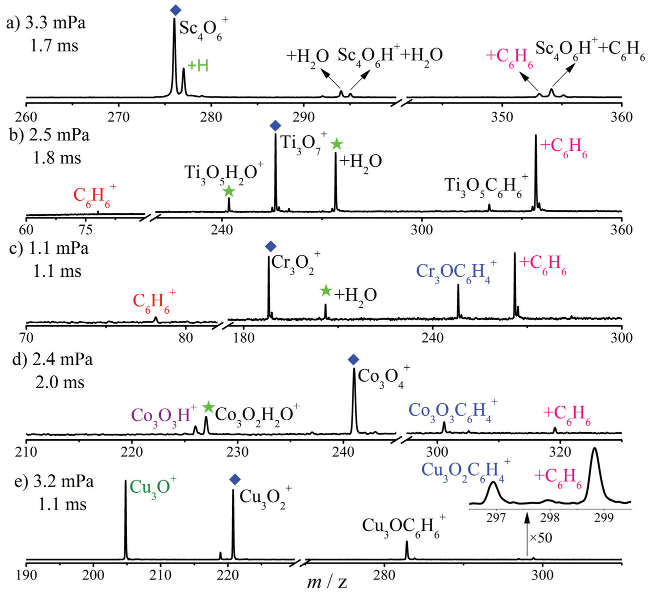

Fig. 1. Time-of-flight mass spectra for the reactions of the mass-selected $Sc_4O_6^+$ (a), $Ti_3O_7^+$ (b), $Cr_3O_2^+$(c), $Co_3O_4^+$(d) and $Cu_3O_2^+$(e) with C_6H_6, respectively. The reaction time and the C_6H_6 pressures are given. The peaks marked with stars are present in the background spectra.

Table 1
Products, *pseudo*-first-order rate constants, and reaction efficiencies for the investigated reactions.

Reactions	Products/Equations	Branching ratios	k_1 (cm^3 $molecule^{-1}$ s^{-1})	Φ
$Sc_4O_6^+ + C_6H_6$	$Sc_4O_6H^+ + C_6H_5^•$	89% (1a)	$(4.2 \pm 0.9) \times 10^{-10}$	0.44
	$Sc_4O_6C_6H_6^+$	11% (1b)		
$Ti_3O_7^+ + C_6H_6$	$Ti_3O_7 + C_6H_6^+$	1% (2a)	$(9.6 \pm 2.0) \times 10^{-10}$	1.00
	$Ti_3O_5C_6H_6^+ + O_2$	12% (2b)		
	$Ti_3O_7C_6H_6^+$	87% (2c)		
$Cr_3O_2^+ + C_6H_6$	$Cr_3O_2 + C_6H_6^+$	2% (3a)	$(4.0 \pm 0.8) \times 10^{-10}$	0.40
	$Cr_3OC_6H_4^+ + H_2O$	32% (3b)		
	$Cr_3O_2C_6H_6^+$	66% (3c)		
$Co_3O_4^+ + C_6H_6$	$Co_3O_3H^+ + C_6H_5O^•$	25% (4a)	$(1.3 \pm 0.3) \times 10^{-9}$	1.33
	$Co_3O_3C_6H_4^+ + H_2O$	43% (4b)		
	$Co_3O_4C_6H_6^+$	32% (4c)		
$Cu_3O_2^+ + C_6H_6$	$Cu_3O^+ + C_6H_6O$	96% (5a)	$(1.1 \pm 0.4) \times 10^{-9}$	1.11
	$Cu_3O_2C_6H_4^+ + H_2$	1% (5b)		
	$Cu_3O_2C_6H_6^+$	3% (5c)		

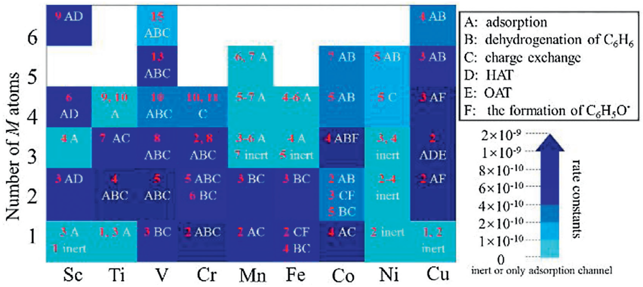

Fig. 2. Map showing of the reactivity and reaction channels for 3d transition metal oxide cations with C_6H_6. The red number shown in each block represents the oxygen atoms y in $M_xO_y^+$ cations. The blank block means these clusters have not been investigated.

Then the formed $C_6H_6^+$ radical cations can further react fast with other atmospheric radicals through radical reactions.

Different from the generally existing pathways 1–3 in Scheme 1a, the HAT process prevails predominantly only in $(Sc_2O_3)_{1-5}^+/C_6H_6$ systems, with the formation of $(Sc_2O_3)_{1-5}H^+$ and C_6H_5 (Fig. 1a and Fig. S1). The $Sc_8O_{12}^+$ is the most reactive one and the BRs for this HAT channel varied from 38% (for $Sc_{10}O_{15}^+$) to 90% (for $Sc_6O_9^+$). As reported in literature, $\Delta \equiv 2y - nx + q$ (q: the charge number, n: the highest oxidation state of element M') can be used to classify oxygen-richness or -poorness of early transition metal oxide clusters $M'_xO_y^q$ [15,57], and the $\Delta = 1$ clusters $(Sc_2O_3)_n^+$, which possess oxygen-centered radicals ($O^{-•}$), can activate the C—H bond of C_4H_{10} [58]. Although the C—H bond energy (BE) of C_6H_6 (4.89 eV) is higher than that of CH_4 (4.55 eV) [59], there is no doubt that $O^{-•}$ plays a key role for the HAT process in $(Sc_2O_3)_n^+$/benzene systems. Larger scandium oxide cluster cations with stoichiometry of $(Sc_2O_3)_n$ may also be able to activate C_6H_6 through HAT, which is not further investigated herein. Among other studied early TMOC cations with $\Delta = 1$, such as $(V_2O_5)_{1-4}^+$ and $(CrO_3)_{1,2}^+$, only $(V_2O_5)_{1-4}^+$ clusters can abstract one hydrogen atom from C_6H_6, and this channel is not the dominant one [50]. Schwarz *et al.* pointed out that an increase or decrease in electronic multiplicity of the bare MO^+ (M = Sc-Ni) coincides with a similar trend in the richness and variety of the products formed in the reactions with C_6H_6 [40]. However, this phenomenon is not suitable for the benzene oxidation on polynuclear metal oxide cation clusters studied herein.

It is interesting that in benzene oxidation reactions with FeO_2^+, $Co_2O_3^+$, $Co_3O_4^+$, $Cu_2O_2^+$ and $Cu_4O_3^+$ clusters ($M_xO_y^+$), oxygen atom transfer accompanying HAT happens, leading to the formation of $C_6H_5O^•$ radicals and $M_xO_{y-1}H^+$ cations [60]. Note that the bond dissociation energies of FeO^+, CoO^+, and CuO^+ are relatively weak in the first-row transition metal monoxide ions MO^+ [61]. According to the thermodynamic requirement that must be met by these $M_xO_y^+$, the reactive M—O bond energies for $M_xO_y^+$ should be within this range: $BE(M–O) < BE(C_6H_5–O)-BE(C_6H_5–H) = (8.126–4.896)$ eV = 3.23 eV (The bonds energy for C_6H_5–O is calculated at the B3LYP/6-311++G** level of theory, and that for C_6H_5–H is from Ref. [60]). Besides, we systematically studied the reactions of nanosized vanadium oxide cluster cations with benzene, and phenol is the product; surprisingly, the size is not the major factors influencing the clusters' reactivities [50].

In the atmosphere, $OH^•$ radicals are one of the most important oxidant, and there are lots of products observed from the $OH^•$ radical-initiated reactions of benzene [62], which leads to the removal of benzene and other VOC molecules from the atmosphere or transformation in the atmosphere. For instance, in Scheme 1b, the abstraction pathway can form H_2O and a phenyl radical in $OH^•$/benzene system, accounting for 5% of the overall reaction at 298 K [63,64]. The $C_6H_5^•$ radical can further react with O_2 to produce $C_6H_5O^•$ ($C_6H_5^• + O_2 \rightarrow C_6H_5O^• + O$, Progress (2)). The following reaction $C_6H_5O^• + M \rightarrow C_5H_5^• + CO + M$ (Progress (3)) will obtain cyclopentadienyl ($C_5H_5^•$) radical, which is a key intermediate species for aromatic ring growth [65]. Phenol is also generated *via* $OH^•$ addition reaction to benzene (Progress (4)). Three (intermediate) products for $OH^• + C_6H_6$ were also observed in our gas-phase model reactions, such as $C_6H_5^•$ radical, $C_6H_5O^•$ radical, and C_6H_5OH. In contrast, H_2O is formed through breaking of two C—H bonds in benzene and generating of C—O bonds in cluster reactions, and this dehydrogenation channel is generally present with large BRs. Therefore, the mechanisms and BRs of dehydrogenation in benzene oxidation reactions mediated by $OH^•$ radical and 3d TMOC cations are different. Physical adsorption by mineral dusts is the one of major sinks for VOC molecules [65], and the adsorption channels are also generally present in most of the investigated cluster cations. Based on the cluster reactions, other two types of channels existing in gas-phase cluster/C_6H_6 systems, that is, charge exchange and dehydrogenation, may contribute to the corresponding VOC oxidation reactions in the atmosphere. From these results, we may speculate that similar reaction types observed in $OH^• + C_6H_6$ in the atmosphere may also exist in the heterogeneous reactions of benzene molecules over mineral dusts, but the mechanisms and importance of each channels may be different; there are also some specific reactions on mineral oxide surfaces, which are not present in the gas-phase reaction of $OH^•$ with C_6H_6. These ring-retaining radical products obtained in the benzene oxidation reactions can further react with other radicals or species in the atmosphere.

In summary, we systematically investigate 103 reactions of small 3d transition metal oxide cations with C_6H_6 by using mass spectrometry, and a clear picture of the reactivity of TMOCs toward benzene is built. As summarized in Fig. 2, a total of 39 cations can oxidize C_6H_6 efficiently, with the rate constants being in the order of 10^{-9}–10^{-10} cm^3 $molecule^{-1}$ s^{-1}, regardless of adsorption channel. The shade of color indicates the approximate range of reaction rates. And the darker the color, the faster the reaction. The blank block means these clusters have not been investigated. As shown in Fig. 2, In the obtained six primary reaction channels, dehydrogenation of benzene and charge transfer between cations and C_6H_6 generally exist in the investigated reactions, and the formation of $C_6H_6O^+$ has not been reported previously. In comparison with hydroxyl radical, the most important gas-phase oxidant in the atmosphere, three (intermediate) products are observed in the reactions of TMOCs with benzene, that is, $C_6H_5^{\bullet}$ radical, $C_6H_5O^{\bullet}$ radical, and phenol. The reaction information is particularly valuable for gauging of future nano- and multiscale modeling of benzene oxidation over mineral oxide aerosols in the atmosphere, and one may expect that the heterogeneous conversion of VOCs such as C_6H_6 on mineral dusts is indispensable.

Acknowledgments

This work was supported by National Key R&D Program of China (No. 2016YFC0203000), the National Natural Science Foundation of China (No. 21503015), and the Fundamental Research Funds for the Central Universities (Nos. 22050205, 2017CX01008).

Appendix A. Supplementary data

Supplementary data associated with this article can be found, in the online version, at https://doi.org/10.1016/j.cclet.2019.05.015.

References

[1] J.G. Calvert, R. Atkinson, K.H. Becker, et al., The Mechanisms of Atmospheric Oxidation of Aromatic Hydrocarbons, Oxford University Press, New York, 2002.
[2] C.R. Usher, A.E. Michel, V.H. Grassian, Chem. Rev. 103 (2003) 4883–4939.
[3] T. Kameda, E. Azumi, A. Fukushima, et al., Sci. Rep.—UK 6 (2016) 1–10.
[4] J.L. Jimenez, M.R. Canagaratna, N.M. Donahue, et al., Science 326 (2009) 1525–1529.
[5] E. Borrás, L.A. Tortajada-Genaro, Atmos. Environ. 47 (2012) 154–163.
[6] G. Wang, R. Zhang, M.E. Gomez, et al., Proc. Natl. Acad. Sci. U. S. A. 48 (2016) 13630–13635.
[7] M. Kalberer, D. Paulsen, M. Sax, et al., Science 303 (2004) 1659–1662.
[8] B. Zheng, Q. Zhang, Y. Zhang, et al., Atmos. Chem. Phys. 14 (2015) 2031–2049.
[9] J. Duan, J. Tan, Atmos. Environ. 74 (2013) 93–101.
[10] H.Z. Tian, C.Y. Zhu, J.J. Gao, et al., Atmos. Chem. Phys. 15 (2015) 12107–12166.
[11] H.J. Tong, P.S.J. Lakey, A.M. Arangio, et al., Faraday Discuss. 200 (2017) 251–270.
[12] H. Schwarz, Catal. Sci. Technol. 7 (2017) 4302–4314.
[13] H. Schwarz, S. Shaik, J.L. Li, J. Am. Chem. Soc. 139 (2017) 17201–17212.
[14] S.M. Lang, T.M. Bernhardt, Phys. Chem. Chem. Phys. 14 (2012) 9255–9269.
[15] X.L. Ding, X.N. Wu, Y.X. Zhao, et al., Acc. Chem. Res. 45 (2012) 382–390.
[16] R.A.J. O'Hair, G.N. Khairallah, J. Cluster Sci. 15 (2004) 331–363.
[17] J. Roithová, D. Schröder, Chem. Rev. 110 (2010) 1170–1211.
[18] A.W. Castleman Jr., Catal. Lett. 141 (2011) 1243–1253.
[19] S. Yin, E.R. Bernstein, Int. J. Mass Spectrom. 321–322 (2012) 49–65.
[20] N. Dietl, M. Schlangen, H. Schwarz, Angew. Chem. Int. Ed. 51 (2012) 5544–5555.
[21] D. Caraiman, G.K. Koyanagi, D.K. Bohme, J. Phys. Chem. A 108 (2004) 978–986.
[22] P. Cheng, A. Shayesteh, D.K. Bohme, Cheminform 40 (2010) 241–246.
[23] G.K. Koyanagi, D.K. Bohme, Int. J. Mass Spectrom. 227 (2003) 563–575.
[24] X.P. Xing, Z.X. Tian, H.T. Liu, et al., Rapid Commun. Mass Spectrom. 17 (2003) 1743–1748.
[25] T. Hanmura, M. Ichihashi, T. Kondow, J. Phys. Chem. A 106 (2002) 11465–11469.
[26] T. Kurikawa, H. Takeda, M. Hirano, et al., Organometallics 18 (2012) 1430–1438.
[27] D. Caraiman, D.K. Bohme, J. Phys. Chem. A 106 (2002) 9705–9717.
[28] D.J. Trevor, R.L. Whetten, D.M. Cox, et al., J. Am. Chem. Soc. 107 (1985) 518–519.
[29] M.R. Zakin, D.M. Cox, R.O. Brickman, et al., J. Phys. Chem. 93 (1989) 6823–6827.
[30] Y. Huang, B.S. Freiser, J. Am. Chem. Soc. 112 (1990) 1682–1685.
[31] X.P. Xing, H.T. Liu, Z.C. Tang, PhysChemComm 6 (2003) 32–35.
[32] C. Berg, M. Beyer, U. Achatz, et al., J. Chem. Phys. 108 (1998) 5398–5403.
[33] S. Roszak, D. Majumdara, K. Balasubramaniana, J. Phys. Chem. A 103 (1999) 5801–5806.
[34] X.P. Xing, Z. Tian, H.T. Liu, et al., J. Phys. Chem. A 107 (2003) 8484–8491.
[35] H.T. Liu, S.T. Sun, X.P. Xing, et al., Rapid Commun. Mass Spectrom. 20 (2006) 1899–1904.
[36] M. Tombers, L. Barzen, G. Niednerschatteburg, J. Phys. Chem. A 117 (2013) 1197.
[37] Y.P. Ho, R.C. Dunbar, Int. J. Mass Spectrom. 182–183 (1999) 175–184.
[38] R.C. Dunbar, G.T. Uechi, B. Asamoto, J. Am. Chem. Soc. 116 (1994) 2466–2470.
[39] L. Barzen, M. Tombers, C. Merkert, et al., Int. J. Mass Spectrom. 330–332 (2012) 271–276.
[40] M.F. Ryan, D. Stoeckigt, H. Schwarz, J. Am. Chem. Soc. 116 (1994) 9565–9570.
[41] C. Heinemann, H.H. Cornehl, D. Schroder, et al., Inorg. Chem. 35 (1996) 2463–2475.
[42] F. Dong, S. Heinbuch, Y. Xie, et al., J. Am. Chem. Soc. 131 (2009) 1057–1066.
[43] K.A. Zemski, R.C. Bell, A.W. Castleman, Int. J. Mass Spectrom. 184 (1999) 119–128.
[44] B. Butschke, H. Schwarz, Organometallics 30 (2011) 1588–1598.
[45] K. Judai, M. Hirano, H. Kawamata, et al., Chem. Phys. Lett. 270 (1997) 23–30.
[46] G.S. Jackson, F.M. White, C.L. Hammill, et al., J. Am. Chem. Soc. 119 (1997) 7567–7572.
[47] Z.Y. Li, Z. Yuan, X.N. Li, et al., J. Am. Chem. Soc. 136 (2014) 14307–14313.
[48] G. Kummerlöwe, M.K. Beyer, Int. J. Mass Spectrom. 244 (2005) 84–90.
[49] T. Su, M.T. Bowers, J. Chem. Phys. 58 (1973) 3027–3037.
[50] J.T. Cui, Y. Zhao, J.C. Hu, et al., J. Chem. Phys. 149 (2018) 074308.
[51] S.M. Lang, D.M. Popolan, T.M. Bernhardt, Chem. Phys. Solid Surf. 12 (2007) 53–90.
[52] M. Arenz, S. Gilb, U. Heiz, Chem. Phys. Solid Surf. 12 (2007) 1–51.
[53] Y.X. Zhao, X.N. Wu, Z.C. Wang, et al., Chem. Commun. 46 (2010) 1736–1738.
[54] S. Detlef, S. Helmut, Helv. Chim. Acta 75 (1992) 1281–1287.
[55] H. Higashide, T. Oka, K. Kasatani, et al., Chem. Phys. Lett. 163 (1989) 485–489.
[56] N.S. Shuman, D.E. Hunton, A.A. Viggiano, Chem. Rev. 115 (2015) 4542.
[57] Y.X. Zhao, X.N. Wu, J.B. Ma, et al., Phys. Chem. Chem. Phys. 13 (2011) 1925–1938.
[58] X.N. Wu, B. Xu, J.H. Meng, et al., Int. J. Mass Spectrom. 310 (2012) 57–64.
[59] Y.R. Luo, Comprehensive Handbook of Chemical Bond Energies, CRC Press, Boca Raton, 2007.
[60] J.T. Cui, C.X. Sun, Y. Zhao, et al., Phys. Chem. Chem. Phys. 21 (2019) 1117–1122.
[61] D. Schröder, H. Schwarz, Angew. Chem. Int. Ed. 34 (1995) 1973–1995.
[62] R. Atkinson, J. Arey, Chem. Rev. 103 (2003) 4605–4638.
[63] R. Atkinson, J. Phys. Chem. Ref. Data 26 (1997) 215–290.
[64] T. Seta, M. Nakajima, A. Miyoshi, J. Phys. Chem. A 110 (2006) 5081–5090.
[65] X. Shen, Y. Zhao, Z. Chen, et al., Atmos. Environ. 68 (2013) 297–314.